POLITECNICO
MILANO 1863

SCUOLA DI INGEGNERIA INDUSTRIALE
E DELL'INFORMAZIONE

Executive Summary of the Thesis

Mathematical modelling and parameter classification for symmetric- and full-cell batteries with metallic anodes

Laurea Magistrale in Energy Engineering - Ingegneria energetica

Author: Chiara Marino

Advisor: Prof. Benedetto Bozzini

Co-advisor: Dott.ssa Elisa Emanuele, Prof.ssa Ivonne Sgura

Academic year: 2025-2026

1. Introduction

Driven by the global demand for safe and sustainable energy storage, this work addresses the technical limitations of aqueous zinc batteries—primarily dendritic growth and surface passivation—by moving beyond conventional integral descriptors toward a physics-based interpretation of voltage-time transients. The research develops a comprehensive model for Zn–Ni full cells by extending the Metal Anode Charging (MAC) framework via the two-parameter Margules formalism, thereby establishing a thermodynamically consistent description of the asymmetric competition between morphology-driven anode dynamics and solid-state cathode intercalation. By coupling this model with an automated waveform classification algorithm, the work enables the systematic mapping of distinct voltage profiles to specific multidimensional admissible regions in the parameter space, directly linking measurable electrical signals to underlying physical characteristics. This approach effectively transforms voltage morphology into a quantitative diagnostic tool, providing a foundation for the future integration of machine learning and operando monitoring to turn electrical fingerprints into predictive indicators of the internal state and degradation pathways of practical zinc-based energy storage systems.

2. Mathematical Framework: From the Classical MAC Model to Full-Cell Extension

The theoretical foundation of this thesis is the Metal Anode Charging (MAC) model[1, 4], a mathematical framework based on coupled partial differential equations (PDEs) designed to describe the response of symmetric electrochemical cells. Operating within a 1D electrolyte domain, the model links measured cell voltage transients with internal electrode shape evolution—specifically dendrite formation and surface passivation—by calculating the metal-ion concentration $u(x,t)$ and the electrolyte potential $\phi(x,t)$.

A significant contribution of this work is the extension of the MAC model to Ni-Zn full-cell configurations [3]. This was achieved modifying the boundary conditions (BCs) at the cathode interface ($x = L$). While the zinc anode remains governed by morphology-driven phenomena and kinetics, we introduced a new governing equation for the Ni/NiOOH cathode based on the

two-parameter Margules (TPM) formalism [2]. An extension of these model provides a thermodynamic description of the non-ideality based on the solid-state mixture, treating the oxidized and reduced nickel species as distinct components of a binary solid solution. The foundation of this model lies in the Gibbs free energy of mixing ΔG_{mix} which, for non-ideal systems, is expressed as the sum of three components[2]:

$$\Delta G_{\text{mix}} = \Delta G_{\text{id}} + \Delta G_R + \Delta G_{\text{ex}} \tag{1}$$

This method expands the excess energy into a power series of mole fractions, where the coefficients represent effective molecular sizes and interaction parameters (including binary and ternary interactions). The final expretion of the potential for the new boundry condition of the MAC model is obatined by deriving the total Gibbs free energy, obtaining:

$$\begin{aligned} V = E_0 + \frac{RT}{F} \ln\left(\frac{t-\alpha}{t+\beta}\right) \\ + \frac{RT}{2F}\Big(-2A + 4A(1-t) - 2B + 6B(1-t) \\ - 3B(1-t)^2 + C(1-t)^3\Big) \end{aligned} \tag{2}$$

3. Cell voltage transient classification

An exhaustive inspection of the experimental voltage time series was performed prior to any model-based interpretation, with the objective of identifying recurring qualitative shapes in the galvanostatic transients. Rather than fitting individual curves, the work takes on a regime-based strategy centered on waveform morphology. Rather than targeting the exact reconstruction of individual voltage curves, the analysis focuses on the classification of transient morphologies and on the determination of the corresponding admissible regions in parameter space. In this framework, each characteristic waveform is associated not with a single parameter vector, but with a finite multidimensional domain, as a hypervolume, within the space of governing parameters.

3.1. Symmetric cell shape classification

Each half-cycle of the symmetric cell transient, was examined independently: this systematic inspection revealed that the vast majority of experimental responses can be classified into four fundamental transient morphologies.
Shape 1 – Single Minimum. This waveform is characterized by an initial decrease in voltage reaching a well-defined minimum, followed by a recovery toward higher values within the same semi-period. Shape 2 – Extremum Reversal (Minimum–Maximum or Maximum). This morphology exhibits the presence of two distinct curvature regions, typically a minimum followed by a maximum, or in some cases a pronounced maximum alone. Shape 3 – Monotonically Increasing Profile. In this case, the voltage increases continuously throughout the semi-period without internal extrema. Shape 4 – Monotonically Decreasing Profile. This transient is characterized by a continuous voltage decrease over the entire semi-period.

3.2. Full cell shape classification

The same analysis was then extended to the full model configuration, taking into account that the full Zn–Ni cells introduces an intrinsic asymmetry between charge and discharged transient, absent in the symmetric configuration, so it was necessary to look at the charge and discharge curve indipendently.
The morphological classification for full-cell transients reveals that Shape 3 is the predominant configuration, appearing with high regularity in both positive and negative semi-periods. It is important to notice taht, in experiments utilizing the TQC cathode, Shape 3 appears with a high degree of symmetry across both positive and negative semi-periods. Shape 4 is generally observed during negative transients but remains significantly less recurrent than Shape 3 in the experimental datasets. Finally, Shapes 1 and 2 are rare within the full-cell framework, appearing only within limited regions of the parameter space or under specific operating conditions.

3.3. Algorithm for shape recognition of voltage transients

To automate classification, a MATLAB-based algorithm is developed. Each semi-period is divided into six equal sub-intervals, and the average derivative in each interval is computed. The sign pattern of these derivatives is used in a rule-

based logic to assign the waveform to one of the four morphological classes. Additional threshold criteria identify short-circuit events (Shape 5) and passivation conditions (Shape 6); some example are reported in Fig. 2 These models were suited to both symmetric and full cell configuration with the only difference that, in the full model, we had to split the positive and negative period in two different plots, to better identify possible asymmetries, as shown in Fig. 3
This approach enables high-throughput, reproducible classification of large experimental datasets and, each experiment, was classiefied accordig to the prevealent charateristic shape of the voltage transient.

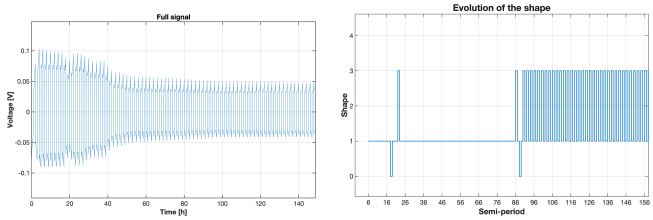

Figure 1: NDSB-201

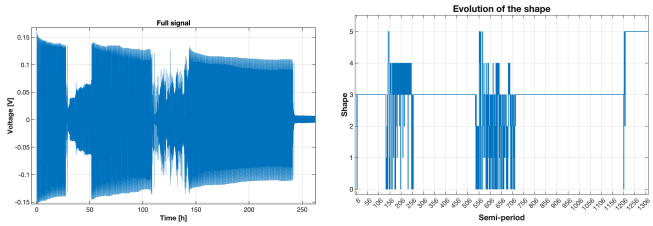

Figure 2: Laser cut

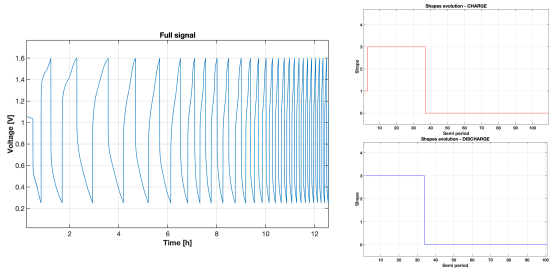

Figure 3: DESEG 50%

3.3.1 Experimental validation with symmetric cells

Gemini ha detto The automated classification of voltage transients establishes a direct mapping between waveform morphology and underlying physical regimes, where Shape 1 identifies stable, regulated mass transport and the transition from shape 1 to Shape 3 signifies a transition to diffusion-limited conditions caused by progressive surface roughening. Zwitterionic additives such as NDSB-257 and NDSB-201, stabilize these transients by utilizing aromatic moieties to selectively adsorb at dendrite tips, increasing the cells time to failure; however, this regulation is compromised at higher passivation phenomena towards the end of mensuration. While standard operation across various fabrication methods is dominated by Shape 3, post-failure states transition to Shape 4 charcterized by a parameter B almoste equal to 0, reflecting a resistive regime governed by ZnO dielectric layers and negligible charge-transfer kinetics. An additional set of data on different aqueous electrolytes, and different cathode, was also an- alyzed to enhance the generality and robustness of the proposed model and the associated mor- phological classification framework

3.3.2 Experimental validation with full cells

The analysis of full-cell configurations featuring Zinc (Zn) anodes, and differents cathode, highlights significant differences in transient dynamics depending on the cathode chemistry. In Zn-Ni systems, the electrochemical response is characterized by an intrinsic asymmetry between the charge and discharge semi-periods.
Conversely, cells employing organic cathodes, such as TQC, exhibit highly symmetric voltage transients. In these configurations, Shape 3 remains the consistent waveform for both anodic and cathodic processes throughout the entire cycling life. The organic cathode does not introduce additional curvature signatures or alter the transient dynamics, resulting in a monotonic evolution.

4. Shape transient classification for MAC model solution

While the morphological classification in Section 3.1 was based solely on experimental voltage transients, the next step is to verify if these waveform families can be reproduced by the physics-based Metal Anode Charging (MAC) model. The objective is to verify whether the same four waveform families identified exper-

imentally (Shapes 1–4) also emerge from the physics-based model, and to determine the corresponding regions of parameter space responsible for their generation for both symmetric and full cells. As shown in fig. 4 the MAC model is able to fully represent the voltage transition.

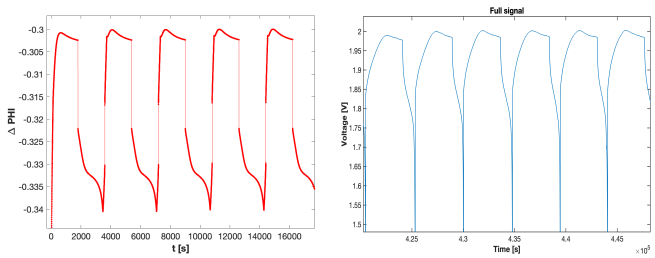

Figure 4:
RED CURVE: MAC model
BLUE CURVE: hot pressed cell

To ensure conceptual clarity and isolate the dominant electrochemical mechanisms, the analysis is deliberately conducted under a simplified and controlled modeling configuration. Specifically, the exploration is restricted to the periodic regime by fixing $FC = 0$ and $K_{\text{pass}} = 0$, thereby neglecting cumulative dendritic growth and passivation effects. Under these assumptions, all deposited metal during the cathodic semi-period is fully removed during the anodic semi-period, and no progressive loss of active surface area occurs.

Before extending the analysis to a global mapping, a local single-parameter sensitivity analysis was conducted using a one-factor-at-a-time approach. By perturbing each governing parameter individually while keeping the others at their reference values, it was possible to directly assess the relative impact of single physical variables on the transient evolution and to evaluate the structural robustness of the corresponding morphological families. The results of these individual parameter variations are illustrated in the subsequent figure, highlighting how specific kinetic or transport constraints uniquely shape the voltage profile.

Once all waveform shapes had been identified, the analysis was extended to a more general framework by systematically mapping the different shapes morphologies obtained through random variations of the governing model parameters (Fig.6). Instead of seeking a unique optimal parameter set, this approach explores the parameter space in a distributed manner, allowing the identification of multidimensional admissible regions (hypervolumes) associated with each transient morphology.The parameter space was delimited by varying each governing variable within a range of plus or minus one order of magnitude from its reference value. This logarithmic perturbation ensures a comprehensive exploration of the transition between transport-limited and kinetics-controlled regimes, while maintaining the model within physically plausible domains. Within this regime-based perspective, every characteristic waveform is not linked to a single parameter vector, but rather to a finite region in the space of transport coefficients, kinetic constants, and geometric descriptors. Each morphology therefore represents a distinct class of electrochemical behavior emerging from specific combinations of physically meaningful parameters [4].

This approach provides two key outcomes: first, it validates the ability of the MAC framework to reproduce the qualitative diversity observed experimentally, second, it establishes a systematic correlation between the transient waveform

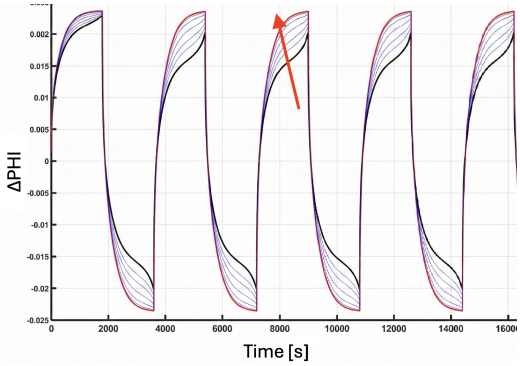

Figure 5: r_{max} sensitivity analysis: progressive shift from shape 3 to shape 2.

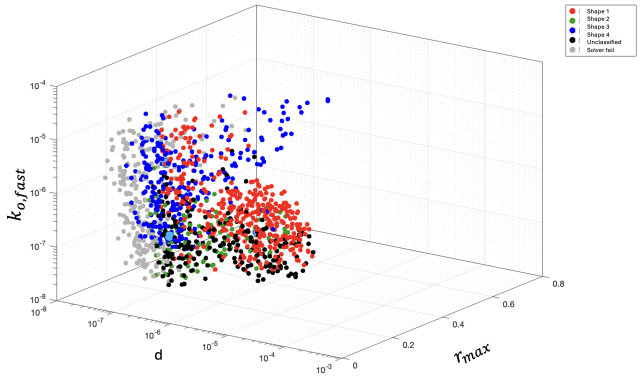

Figure 6: Parameter space mapping of waveform classification with fixed value of B and i_0

morphology and the underlying physicochemical processes, including mass transport phenomena, electrochemical kinetics, and morphological or irreversible changes occurring within the cell[1]. The final results are reported in the tables:

Symmetric model	r_{max}	d	K_{0fast}
SHAPE 1	Medium-small	high	Medium-high
SHAPE 2	small	small	small
SHAPE 3	Small-high	small	high

Table 1: Summary of symmetric model parameters for different shapes.

Full model	**Polarity**	r_{max}	d	K_{0fast}
SHAPE 3	positive	small	small	small
SHAPE 4	positive	small	medium-high	small
SHAPE 3	negative	small	medium-high	small
SHAPE 4	negative	small	small	small

Table 2: Full model parameter comparison for different shapes and polarities.

5. Conclusion

The morphology-based classification and the parameter-space exploration developed in the previous sections provide a structured framework for interpreting the electrochemical behavior of the investigated systems. In this section, the results are discussed from a materials-science perspective, focusing on how electrolyte composition, cathode structure and operating conditions influence the distribution of voltage transient shapes.

5.1. Symmetric Zn–Zn Cells with Zwitterionic Additives

The classification of voltage transients in symmetric Zn-Zn cells utilizes specific waveforms as diagnostic signatures of the physical state of the electrodes. Shape 1 represents a stable electrochemical environment characterized by regulated mass transport and high diffusion coefficients. A transition from Shape 1 to Shape 3 indicates a shift toward diffusion-limited conditions caused by surface roughening and the accumulation of dead metal, which alters local electric fields. Among the additives tested, NDSB-201 and NDSB-257 demonstrated superior performance compared to NDSB-195. This is attributed to their aromatic moieties and high molecular polarizability, which allow for selective adsorption at high-field regions like dendrite tips, thereby increasing local charge-transfer resistance and suppressing localized current density to promote more uniform growth.

5.2. Cells with Different Electrode Cutting Techniques

Symmetric cells produced through mechanical punching, shielded punching, and laser cutting display significant morphological consistency, with Shape 3 serving as the dominant profile during standard operation. Following short-circuit events, the system typically transitions to Shape 4, characterized by irregular transients and voltage spikes. These electrical signatures result from the formation of ZnO layers that function as insulating dielectrics, causing the cell to behave like an RC circuit. This state emerges when charge-transfer kinetics become negligible, specifically as the activation parameter B approaches zero. The subsequent alternation between Shape 3 and Shape 4 reflects a regime of high electrochemical instability and labile short-circuiting, where fragile dendritic contacts intermittently establish and break.

5.3. Symmetric Cells with DES Electrolyte

Symmetric Zn-Zn cells employing deep eutectic solvent electrolytes exhibit a fundamental shift in electrochemical behavior, with Shape 3 appearing as the nearly universal transient morphology. This is physically consistent with the high viscosity of the medium, which reduces the effective diffusion coefficient of zinc ions. The addition of TBAB introduces further complexity, resulting in an alternating sequence of Shape 1 and Shape 3 profiles. This behavior suggests an asymmetric distribution of the additive across the electrode interfaces, which creates divergent kinetic regimes and varying transport characteristics within the cell.

5.4. Full Cells with Zn Anode and Ni cathode

The analysis of nickel-based full-cell configurations shows a notable asymmetry in Shape 3 between the positive and negative semi-periods is often observed, particularly in blade-coated electrodes, due to variations in electrolyte accessibility caused by the specific electrode architecture. While some designs maintain initial symmetry, the onset of failure is characterized by a transition to Shape 2 during the charging cycle. This evolution is mathematically described by an increase in the kinetic parameter k_{0fast} which physically signifies the intensification of the electric field at dendritic tips, leading to localized and aggressive electrodeposition compared to the discharge phase.

5.5. Full Cells with Zn Anode and TQC cathode

Conversely, cells employing TQC cathodes display a characteristic symmetry in Shape 3 voltage profiles both on charge and discharge semi periods, charcterized by low value of d and high value of i0.This combination provides a robust physical explanation for the observed stability that previously seemed counterintuitive. While the low d value (due to high DES viscosity) induces the monotonic potential increase typical of Shape 3, the high i_0 ensures that the interfacial kinetics remain fast and balanced. This equilibrium stabilizes the transients and prevents the amplification of dendritic instabilities, promoting a more durable cycling environment compered to the aqueous solutions.

6. Conclusions

This work establishes a physics-based framework for interpreting voltage transients in aqueous zinc batteries by integrating the Metal Anode Charging (MAC) model with automated waveform classification. A major contribution is the extension of this model to Zn–Ni full cells via the Margules formalism, which successfully captures charge-discharge asymmetries and electrode kinetics. Crucially, the research demonstrates that each distinct waveform shape can be mapped to specific admissible regions within the parameter space, thereby associating transient morphologies with defined physical characteristics and electrochemical regimes. This mapping moves beyond simple curve fitting, allowing measurable electrical signatures to be directly linked to underlying phenomena such as ionic transport limitations, dendritic growth, and passivation. Ultimately, this transforms voltage morphology into a quantitative diagnostic tool, setting the stage for future integration with machine learning and operando diagnostics to monitor the internal state of electrochemical systems.

References

[1] Benedetto Bozzini, Elisa Emanuele, Jacopo Strada, and Ivonne Sgura. Mathematical modelling and parameter classification enable understanding of dynamic shape-change issues adversely affecting high energy-density battery metal anodes. *Applications in Engineering Science*, 13:100125, 2023.

[2] Mukul Jain, Amanda L. Elmore, Michael A. Matthews, and John W. Weidner. Thermodynamic considerations of the reversible potential for the nickel electrode. *Electrochim. Acta*, 43(18):2649–2660, 1998.

[3] Maria Grazia Quarta, Ivonne Sgura, Massimo Frittelli, Raquel Barreira, and Benedetto Bozzini. Shape classification of battery cycling profiles via k-means clustering based on a sobolev distance. *Journal of Computational and Applied Mathematics*, 483:117365, 2026.

[4] Francesca Rossi, Lucia Mancini, Ivonne Sgura, Marco Boniardi, Andrea Casaroli, Alexander Peter Kao, and Benedetto Bozzini. Insight into the cycling behaviour of metal anodes, enabled by x-ray tomography and mathematical modelling. *ChemElectroChem*, 2022.